Available online at www.sciencedirect.com

ScienceDirect

IFAC Papers Online CONFERENCE PAPER ARCHIVE

IFAC PapersOnLine 56-2 (2023) 7802–7807

Multi-Objective Model-Predictive Control for Dielectric Elastomer Wave Harvesters

Matthias K. Hoffmann * **Lennart Heib** * **Gianluca Rizzello** ** **Giacomo Moretti** *** **Kathrin Flaßkamp** *

* *Systems Modeling and Simulation, Saarland University, Saarbrücken, Germany (e-mail: {matthias.hoffmann, kathrin.flasskamp}@uni-saarland.de, lennartheib@gmail.com)*

** *Adaptive Polymer Systems, Saarland University, Saarbrücken, Germany.*

*** *Department of Industrial Engineering, Università di Trento, Italy.*

Abstract: This contribution deals with multi-objective model-predictive control (MPC) of a wave energy converter (WEC) device concept, which can harvest energy from sea waves using a dielectric elastomer generator (DEG) power take-off system. We aim to maximise the extracted energy through control while minimising the accumulated damage to the DEG. With reference to system operation in stochastic waves, we first generate ground truth solutions by solving an optimal control problem, comparing it to the performance of MPC to determine a prediction horizon that trades off accuracy and efficiency for computation. Fixed weights in the MPC scheme can produce unpredictable costs for variable sea conditions, meaning the average rate of cost accumulation can vary vastly. To steer this cost growth, we propose a heuristic to adapt the algorithm by changing the weighting of the cost functions for fulfilling the long-time goal of accumulating a small enough damage in a fixed time. A simulated case-study is presented in order to evaluate the performance of the proposed MPC framework and the weight-adaptation algorithm. The proposed heuristic proves to be able to limit the amount of accumulated damage while improving the energy yield obtained with a comparable fixed-weight MPC.

Keywords: Optimal Control, Multi-objective Model-predictive Control, Energy Harvesting, Non-Linear Optimization, Dielectric Elastomer Generators

1. INTRODUCTION

Ocean wave energy is a highly abundant and dense form of renewable energy. Although many different concepts of wave energy converters (WECs) were studied in the past, their high technological complexity and deployment costs have hindered these technologies from being used in the field (Pecher and Kofoed (2017)). One promising approach to overcome these barriers is the use of dielectric elastomer generators (DEGs), i.e. lightweight polymeric generators based on low-cost raw materials, which allow direct conversion of mechanical into electrical energy based on a variable-capacitance principle (Moretti et al. (2020)). In a previous publication, we derived a model-based optimal control for a DEG-WEC subject to sinusoidal regular waves (see Hoffmann et al. (2022)). We showed that multi-objective optimal control can, under consideration of a non-linear model, disclose technically relevant trade-offs between the electrical damage accumulated by the DEG over time and the extracted energy, allowing for a reduction of damage by more than 50 % while only losing 1 % of energy compared to a control that aims at maximising the extracted energy.

However, these results assumed the wave motion is periodic and predictable far into the future. In reality, ocean waves are irregular and therefore unpredictable for long time-horizons (Coe et al. (2018)). This makes the use of open-loop optimal control difficult, as errors in the prediction of the wave excitation result in suboptimal control signals. Under the assumption that a correct prediction shortly into the future is possible, model-predictive control (MPC) can be used to generate a suitable control signal during operation, having better adaptability to environmental changes than optimal control, while preserving the same cost functions and constraints (Faedo et al. (2017)). The MPC algorithm computes control inputs by solving an optimal control problem (OCP) with a shorter prediction horizon and updating the input estimation on-line, while controls are executed.

In this work, we apply for the first time MPC to DEG-WECs under the influence of stochastic waves. Moreover, we evaluate the deviation of the MPC solution with respect to a ground truth OCP input signal to find that reasonable prediction horizon lengths have to include multiple wave peaks. Additionally, if long-time goals are to be achieved, it is needed that the controller explicitly accounts for the high variability in the system operating conditions. In real-world applications, tracking DEGs damage accumulation enables failure time prediction. This might, among others, allow actively adjusting the controller parameters as the system approaches breakdown, similar to ideas presented by Requate et al. (2022). With this objective in mind,

10.1016/j.ifacol.2023.10.1152

we designed a simple heuristic switching scheme that can adapt the weights in a multi-objective MPC. We show that even a rudimentary switching scheme is effective in limiting the damage accumulation below an arbitrary threshold.

2. MODEL AND PROBLEM STATEMENT

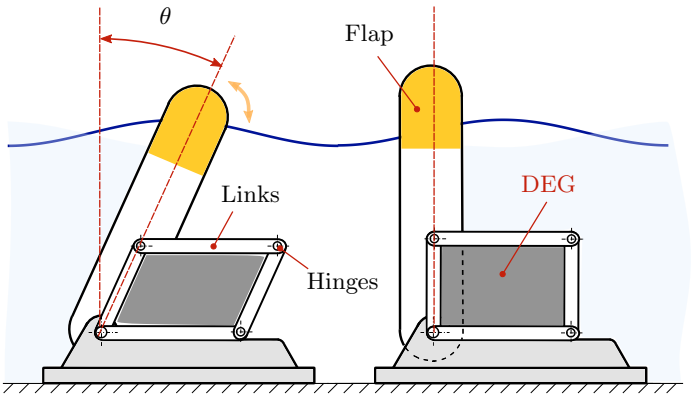

Fig. 1. Wave surge converter: a flap hinged on the sea floor is tilted by the wave motion. It is displayed in a generic (left) and the vertical equilibrium position (right).

2.1 System description

In this work, we design an MPC scheme for the wave surge converter (see, e.g. Whittaker and Folley (2012)), displayed in Fig. 1. The device, hinged to the sea bed, experiences pitch motion due to incoming waves, deforming a DEG composed of electrode-covered polymeric dielectric membranes rigidly connected to a parallelogram mechanism (Moretti et al. (2014)). When no voltage is applied, the DEG generates an elastic torque that pushes the flap towards the vertical equilibrium position $\theta = 0$. Applying a voltage to the DEG adds an electrostatically-induced torque in the same direction as the elastic torque, making the system stiffer. The elastic torque can be considered negligible compared to the electrostatic torque (Moretti et al. (2014)).

The DEG functions as a variable capacitor, which can be controlled so as to generate electrical energy at the expense of the input mechanical work generated by the sea wave moving the flap. Applying low or no voltage during phases where the capacitance increases ($\theta\dot{\theta} < 0$) and a high voltage when the capacitance decreases ($\theta\dot{\theta} > 0$) causes current to flow out of the DEG and electrical power to be delivered to the power electronics. As we showed in our previous work Hoffmann et al. (2022), controlling the input voltage to maximise the energy extracted from the system results in large electric fields, damaging the DEG-material over time and leading to system failure after damage reaches a certain threshold (Chen et al. (2019)). For that reason, we also took the damage into consideration as a second optimization objective and, in turn, consistently limit the electric field in the DEG.

2.2 Model

For small oscillation angles, the dynamics of the wave surge take the following form (Hoffmann et al. (2022)):

$$\begin{aligned}\begin{bmatrix}\dot{\theta}(t)\\ \dot{\delta}(t)\\ \dot{z}(t)\end{bmatrix} &= \begin{bmatrix}0 & 1 & 0^{1\times n}\\ -I_h^{-1}K_\mathrm{h} & -I_\mathrm{h}^{-1}B_\mathrm{h} & -I_\mathrm{h}^{-1}C_\mathrm{r}\\ 0^{n\times 1} & B_\mathrm{r} & A_\mathrm{r}\end{bmatrix}\begin{bmatrix}\theta(t)\\ \delta(t)\\ z(t)\end{bmatrix} +\\ &+ \begin{bmatrix}0\\ I_\mathrm{h}^{-1}\\ 0^{n\times 1}\end{bmatrix}(d(t) - C_0\theta(t)u(t))\\ \theta(0) = \theta_0,\ \delta(0) &= \delta_0,\ z(0) = z_0.\end{aligned} \tag{1}$$

where $\theta(t)$ and $\delta(t) = \dot{\theta}(t)$ from $\mathbb{R}$ describe the flap's angular position and velocity; $z(t) \in \mathbb{R}^n$ is an n-dimensional state vector describing the dynamics of the radiated waves' force (Yu and Falnes (1995)); K_h and B_h represent the hydrodynamic stiffness (due to buoyancy) and damping of the flap; C_0 is the capacity of the undeformed DEG; A_r, B_r, C_r are matrices modelling the radiated waves dynamics; d is a time-varying torque the waves exert on the flap; input u physically represents the voltage v applied on the DEG squared. In the following, the system's state is denoted by $x(t) = [\theta(t), \delta(t), z(t)^\intercal]^\intercal$. In operating conditions, the input $u(t)$ should meet the following hard constraints:

$$0 \leq u(t) \leq (E_\mathrm{bd}h_\mathrm{l})^2, \tag{2}$$

where the first inequality of $0 \leq u$ owes to the definition of u ($u(t) = v(t)^2$), whereas the second constraint demands that the electric field is lower than a threshold breakdown value, E_bd times the DEG's thickness h_l, that would cause static failure of the DEG.

2.3 Cost functions

We aim to simultaneously minimise accumulated damage and maximise extracted energy within a multi-objective optimal control problem (MOOCP) setting. The energy cost function is defined as the energy generated over a time t_f with a negative sign:

$$\begin{aligned}J_1(x,u,t_\mathrm{f}) &= \Psi(x(t_\mathrm{f}),u(t_\mathrm{f}),t_\mathrm{f}) - \Psi(x(0),u(0),0)\\ &+ \int_0^{t_\mathrm{f}}\left(B_\mathrm{h}\delta(t)^2 + z(t)^\intercal S_\mathrm{r} z(t) + \frac{u(t)}{R_0} - d\delta(t)\right)\mathrm{d}t\\ \text{with } \Psi(x(\tau),u(\tau),\tau) &= \frac{1}{2}I_\mathrm{h}\delta(\tau)^2 + \frac{1}{2}K_\mathrm{h}\theta(\tau)^2\\ &+ \frac{1}{2}z(\tau)^\intercal Q_\mathrm{r} z(\tau) + \frac{1}{2}C_0\left(1-\theta(\tau)^2\right)u(\tau),\end{aligned} \tag{3}$$

with the storage function Ψ including kinematic, electrostatic, and hydrostatic energy contributions. R_0 represents the leakage resistance. Q_r and S_r are symmetric matrices satisfying

$$\begin{aligned}S_\mathrm{r} &= -0.5(A_\mathrm{r}^\intercal Q_\mathrm{r} + Q_\mathrm{r}A_\mathrm{r}) \succ 0\\ Q_\mathrm{r} &\succ 0, Q_\mathrm{r}B_\mathrm{r} = C_\mathrm{r}^\intercal,\end{aligned} \tag{4}$$

where $\succ 0$ denotes positive definiteness. Duan and Yu (2013) showed that their guaranteed existence due to the passivity of the system $(A_\mathrm{r}, B_\mathrm{r}, C_\mathrm{r})$.

Dissipation due to viscous, hydrodynamic and electrical losses, and the power input by the incident wave are considered via the integral term in (3). Under the assumptions that the electric field is the main source of damage for the DEG and that damage only starts accumulating if

the electric field exceeds a threshold value E_{th} (Dissado and Fothergill (1992)), the damage cost function can be formulated as

$$J_2(x,u,t_\mathrm{f}) = \alpha \int_0^{t_\mathrm{f}} \left(\max\{u(t) - E_{\mathrm{th}}^2 {h_\mathrm{l}}^2, 0\}\right) \mathrm{d}t, \tag{5}$$

with a normalisation factor α rendering J_2 dimensionless.

Equations (1), (2), (3), and (5) define the MOOCP

Problem 1.

$$\begin{aligned} &\underset{u}{\text{minimise}} \quad (J_1, J_2) \\ &\text{subject to dynamics (1)}, \\ &\qquad 0 \le u(t) \le (E_{\mathrm{bd}} h_\mathrm{l})^2 \quad \forall\, t \in [0, t_\mathrm{f}]\,. \end{aligned} \tag{6}$$

that is solved inside the MPC framework. In the following, the dependence on time t is omitted for brevity.

3. METHODS

3.1 Background on MPC

MPC arose from optimal control as an answer on how to "close the loop" in model-based open-loop optimal control (Rawlings et al. (2017)). In optimal control, a system's behaviour is predicted for a time called the prediction horizon t_f into the future, while optimising the inputs to the system in such a way that a cost function is minimised. The workflow of MPC consists in repeatedly measuring the system's state (or estimating it with an observer), solving an OCP, and feeding the first portion of the calculated inputs to the plant. Fig. 2 qualitatively shows the flap angle, input history, and the predicted state and input that will partially be applied to the system.

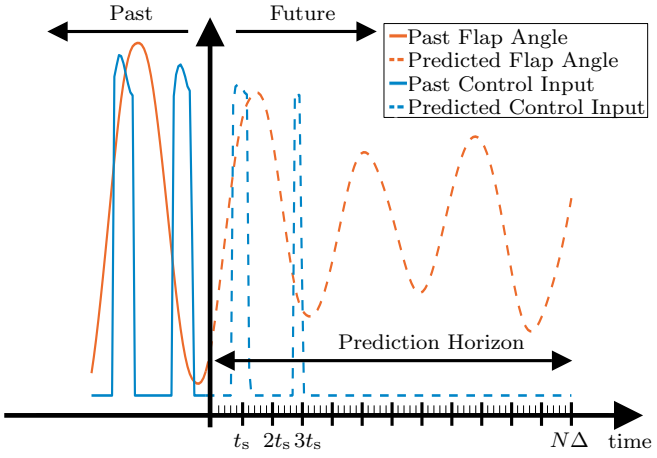

Fig. 2. The MPC working principle on the example of the DEG-WEC. The solid line shows the state and input history, while the dashed line displays the prediction that will be applied to the system partially.

3.2 Discretisation and simplification of the OCP

In order to solve Problem 1, we employ direct methods for optimal control, i.e. the OCP is transcribed into a non-linear program which is then solved by appropriate methods (see Gerdts (2011)). Using gradient-based methods, the discretised optimal control signal is computed. The integral terms inside the cost functions have to be discretised as well. We do so by adding the integrand to the dynamics

$$\begin{aligned} \dot{\Upsilon}_1 &= B_h \delta^2 + z^\intercal S_r z + \frac{u}{R_0} - d\delta \\ \dot{\Upsilon}_2 &= \max\{u - E_{th}^2 h_l^2, 0\}, \end{aligned}$$

with

$$\Upsilon_1(0) = \Upsilon_2(0) = 0.$$

The extended state reads $\xi = [\theta\ \delta\ z^\intercal\ \Upsilon_1\ \Upsilon_2]^\intercal$, with the initial value $\xi_0 = [\theta_0\ \delta_0\ {z_0}^\intercal\ 0\ 0]^\intercal$.

For a time step denoted by Δ and some final time $t_f = N\Delta$, we now introduce a time discretization $\{k\Delta\}_{k=0}^N = \{0, \Delta, 2\Delta, \ldots, N\Delta\}$. In the following, the discretised values corresponding to their continuous counterparts are marked by square brackets, e.g. $\xi[k]$ denotes the extended state k time steps into the future. The current state of the system is advanced by one step into the future using the classical Runge-Kutta-Method of 4th order (RK4), denoted by $F_{\mathrm{RK4}}(\xi[k], u[k], u[k+1], d[k], d[k+1])$. Consecutive values for the input and wave excitation are used to model first-order hold (FOH) behaviour. The dynamics can then be expressed with the equality constraints

$$\begin{aligned} \xi[k+1] = F_{\mathrm{RK4}}(\xi[k], u[k], u[k+1], d[k], d[k+1]) \\ \forall k \in [0, N-2]] \\ \xi[0] = \xi_0. \end{aligned}$$

The cost functions are then $\tilde{J}_1 = \Upsilon_1[N-1]$ and $\tilde{J}_2 = \Upsilon_2[N-1]$, so that the MOOCP is

Problem 2.

$$\begin{aligned} &\underset{u[1],\ldots,u[N]}{\text{minimise}}\ w_1 \tilde{J}_1 + w_2 \tilde{J}_2 \\ &\text{subject to } \xi[k+1] = F_{\mathrm{RK4}}(\xi[k], u[k], u[k+1], \ldots \\ &\qquad d[k], d[k+1]) \forall\ k \in [0, N-2], \\ &\qquad 0 \le u[k] \le (E_{bd} h_l)^2,\ \forall\ k \in [0, N-1] \\ &\qquad \xi[0] = \xi_0 \\ &\qquad u[0] = u_0. \end{aligned} \tag{7}$$

Within the MPC, Problem 7 is solved repeatedly on shifted time intervals and updated initial states. As depicted in Fig. 2, $N\Delta$ becomes the prediction horizon and, let us assume, for the sampling time we have $t_s = r\Delta, r \in \mathbb{N}_{>0}$. The resulting control signal is denoted by u_{MPC}. The values of Ψ are omitted in the formulation. Since $\Psi(0)$ is a constant in the FOH formulation, it does not change the optimization problem. Regarding $\Psi(t_f)$, since $I_\mathrm{h}, K_\mathrm{h}$ are orders of magnitude larger than C_0, their terms dominate the value of Ψ. The quadratic cost terms push the solution to the equilibrium position $\theta = 0$ at the end of the prediction horizon, an effect unwanted in continuous operation, so it is omitted from the energy cost function.

3.3 Generation of the wave excitation profiles

The stochastic wave is modelled as a superposition of a number of n_f sine waves. The amplitude of the different harmonic components has a distribution which for example can be described by the so-called Bretschneider spectrum. The Bretschneider spectrum

$$S_B(\omega) = A_\mathrm{B}\omega^{-5}\exp\left(-B_\mathrm{B}\omega^{-4}\right)$$

describes an average sea state when wave elevation profile measurements are not available, where ω represents an angular frequency. The wave excitation torque

$$d(t) = \sum_{i=1}^{n_\mathrm{f}} \Gamma_\mathrm{F}(\omega_i)A_i(\omega_i)\sin\left(\omega_i t + \phi_i(t)\right).$$

can be calculated from the spectrum, where $\Gamma_\mathrm{F}(\omega)$ is a frequency-dependent excitation coefficient (depending on the hydrodynamics). The coefficients A_i represent the amplitudes of the different harmonic components in the wave profile, given by:

$$A_i = \sqrt{2S_\mathrm{B}(\omega_i)\Delta\omega_i},$$

where $\Delta\omega_i$ are frequency increments, $\phi_i(t)$ are random phase-shifts, and the wave frequencies $\omega_i = \omega_0 + i\Delta\omega\ \forall\ i \in [0, n_\mathrm{f}]$ are linearly increasing. With that, let

$$\omega_\mathrm{f} = \left\{\omega_i \ : \ i = \arg\max_i A_i, i \in [0, n_\mathrm{f}]\right\}$$

be the dominant frequency of the wave. The parameters A_B and B_B can be modified to yield a wave with the desired overall significant wave height, ω_f and frequency profile. For this paper, no specific sea state is emulated. Here, $\phi_i(t)$ are set to change slowly over time so as to prevent the onset of any periodicity in the generated excitation. For the purpose of exemplification, in this paper spectral parameters A_B and B_B are simply chosen in such a way as to keep the resulting trajectories of θ within the model validity bounds, rather than with the aim of representing location-specific sea states.

3.4 Adaptive weight selection

When applying MPC, we do not know exactly how the controlled system will perform cost-wise. Partially responsible for that is the change of what a set of weights means for different sea states. Fig. 3 shows two Pareto fronts (relative to two realisations of the same wave spectrum) for a prediction horizon of 60 s for 15 evenly distributed weights between 0.05 and 0.95. Negative energy corresponds to extracted energy.

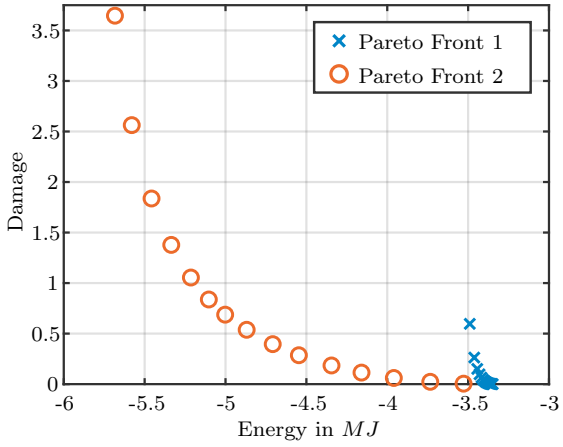

Fig. 3. Pareto fronts relative to two different realisations of a sea state (with same wave spectrum).

In the case of the WEC-DEG, when driving the system with a fixed weighting, different sea states will result in different damage accumulation over time. When the accumulated damage surpasses a certain threshold, the DEG breaks down and needs to be replaced. In a wave farm with multiple DEGs, it might be desirable to render the average expected lifetime of a certain device as close as possible to that of the rest of the farm, in a way that multiple units can be replaced together at once, hence minimising the operational costs. A strategy to extend the (average) expected lifetime of a unit up to a target time t_bd is by changing the weighting of the damage cost function in a way that the accumulated damage cost at time t_bd does not exceed a fixed value J^d (corresponding to a rupture threshold). Let us consider a fixed set $W = \{(w_1^i, w_2^i)\}_{i=1}^{n_\mathrm{w}}$ of n_w weight combinations with increasing values of w_2^i (the weight of damage cost J_2), decreasing values of w_1^i, and an initial weight index $i_\mathrm{w} \in [1, n_\mathrm{w}]$. A way of estimating if the damage goal is achievable with the current weighting is by evaluating the MPC performance over N_p time steps into the past. The average rate of damage accumulation J_ps is estimated and the damage at the break-down time is predicted by assuming that the average damage accumulation trend continues as in the past N_p steps. If the predicted damage exceeds J^d, i_w is decreased by 1, effectively decreasing w_1. Otherwise, if the predicted damage falls below $c_\mathrm{d}J^\mathrm{d}$ with $c_\mathrm{d} \in [0, 1]$, i_w is increased by 1. This is done every N_p steps (provided that the DEG was actuated with non-zero input during that time). We hereby show that this very simple heuristic is effective in providing margins to extend the DEG lifetime, motivating further research on more elaborate adaptation algorithms.

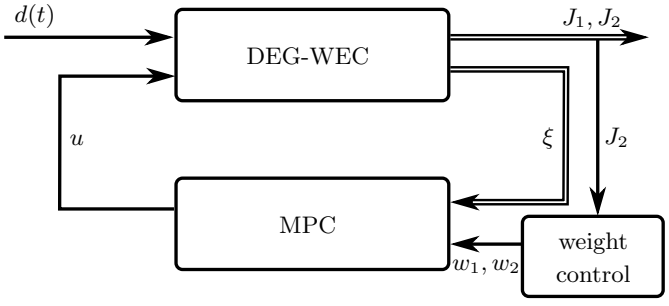

Fig. 4. Schematic of the weight controlled MPC. The weight controller keeps a history of past damage values, projects the estimated damage trend into the future and selects a weighting to be used in the MPC accordingly.

4. NUMERICAL RESULTS

We present numerical implementations of the proposed MPC framework in MATLAB. The numerical data used for the analysis are the same as in Hoffmann et al. (2022). The optimisation problems were formulated and solved using the CasADi package by Andersson et al. (2019) and the IPOPT solver by Wächter and Biegler (2006). The stochastic waves were generated using a superposition of equally-spaced 50 harmonics with a base frequency of 0.1 Hz with $A_\mathrm{B} = 0.0032$ and $B_\mathrm{B} = 0.1054$. The nominal MPC case is assumed.
Examples of MATLAB implementations for the reference DEG-WEC system are available in our Github reposi-

tory, with examples for fixed-weight and weight-controlled MPC [1].

4.1 Accuracy of model-predictive control

Applying MPC will, in general, generate different control trajectories every time the prediction horizon is shifted, due to the new information available. Fig. 5 shows the mean absolute error (MAE), expressed as the L_2 norm of the difference between the ground truth OCP solution over a prediction horizon of 320 s and the control signal obtained from MPC u_{MPC}; u_{MPC} was calculated using different horizon lengths from 10 to 77 s. As expected, the error decreases for longer prediction horizons.

In Fig. 6, we show the control inputs and states for example solutions from different prediction horizons. The ground truth optimal solution is approximated poorly for a prediction horizon of 12 s (left) compared to an accurate tracking for 60 s (right). In all cases, the control has a bang-bang-like behaviour, with voltage being applied on the DEG only during certain time intervals. Short-horizon MPC solutions differ from the ground truth solution in terms of the turn-on and turn-off timings, which are correctly estimated when longer prediction horizons are used. These trends are consistent with heuristic controllers proposed by Moretti et al. (2014), in which a (piecewise constant) input is applied when $\theta\dot{\theta} \geq 0$. Compared to such a heuristic, the MPC leads to complex (non-piecewise-constant) voltage input waveforms. The similarity of the 60 s-MPC solution to the ground truth is also reflected by the extracted energy, which differs from the ground truth value by only 0.5 %. In the following analyses, we will refer to an MPC horizon of 60 s.

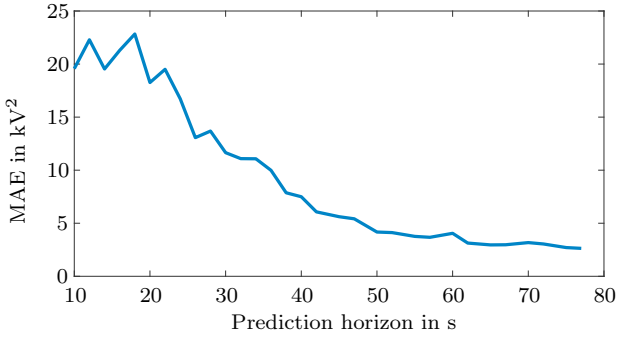

Fig. 5. Deviation of u_{MPC} from ground truth for different prediction horizon lengths. We take the mean error of simulations over a time window of 320 s. Ground truth is an OCP solution over the whole horizon.

4.2 Weight selection algorithm

In this section, we evaluate the performance of the simple heuristic weight selection algorithm presented in section 3.4 by simulating the system's behaviour for different sea states. We used a set of $n_{\mathrm{w}} = 15$ predetermined weights w_2^i, evenly distributed between 0.05 and 0.95, and chose w_1^i such that $w_1^i + w_2^i = 1\ \forall i \in [1, n_{\mathrm{w}}]$.

[1] https://github.com/MKHoffmann/IFAC_WC_2022_WaveHarvestingExample

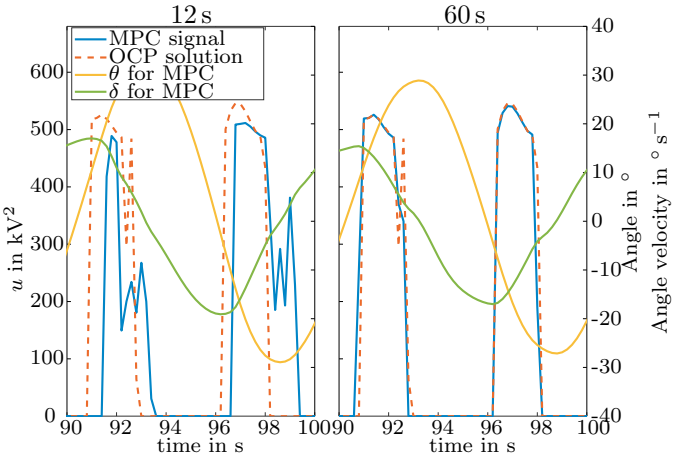

Fig. 6. Comparison of the MPC solutions for prediction horizons of 12 s and 60 s with the ground truth OCP solution.

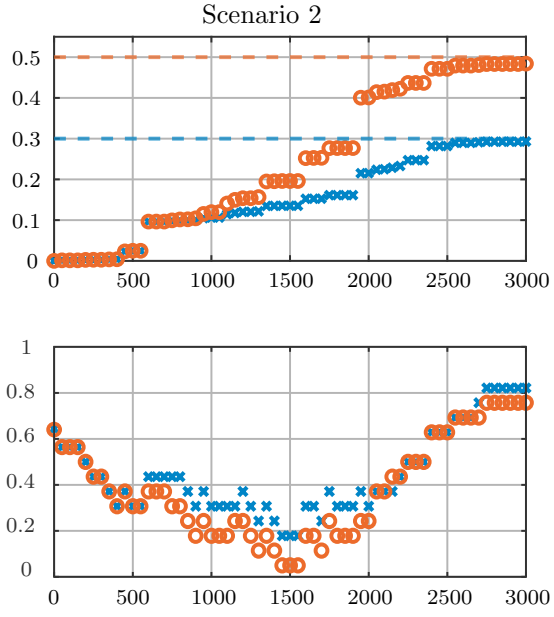

Fig. 7. Evaluation of the MPC with weight controller for an exemplary sea state and two target damage values. For clarity, only every 100th value is displayed. Top: Accumulated damage over time. Bottom: The selected weight index i_{w} over time. A lower index corresponds to a higher weighting for the damage cost.

We compare the performance of the MPC with weight controller for two target damage values $J^{\mathrm{d}} = \{0.3, 0.5\}$. These threshold values (together with target time $t_{\mathrm{bd}} = 3000$ s) are used here for the sole purpose of exemplification and do not reflect real failure thresholds. The performance of a weighting is evaluated every 25 s. An increase in the damage weighting is allowed after each evaluation, whereas a decrease is every two evaluations.

Fig. 7 shows the performance of the heuristic weight control by displaying the accumulated damage in the top and the selected weighting index in the bottom plot. Certain sea states might be characterised by phases during which the excitation d has a small amplitude. In these cases, selecting high values for w_1 might lead to steep damage

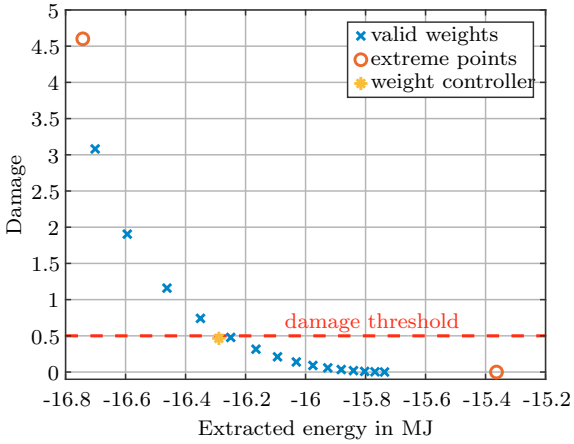

Fig. 8. The accumulated costs for the fixed weight MPC with the valid weights for the weight-controller and the extreme point approximations for the left case from Fig. 7. The costs resulting from the weight controller with a threshold of 0.5 dominate all of the fixed weights costs that follow the damage threshold.

increases when the excitation amplitude suddenly rises. This is shown in Fig. 7, where a sudden increase in damage is recorded at $t = 1800$. At this point, the heuristic controller continually decreases i_w, which allows the damage accumulation to stay below the target threshold.
Remarkably, the difference in extracted energy with the two threshold values for J^d is very small, 0.32 %. To motivate this, we compare the weight-controlled MPC with the fixed-weight MPC. In addition to the 15 weights used in the weight-controller, we also use $w_2 = 0.99$ and $w_2 = 0.01$ to approximate the extreme points that minimise one of the cost functions.

Fig. 8 shows that the difference in extractable energy for fixed weights is less than 6 %. The weight-controlled MPC yields more harvested energy than all fixed-weight MPCs that accumulate damage $J_2 \leq J^\mathrm{d}$ over a time-frame of 3000 s. This is possible thanks to the fact that fixed-weight MPC solutions are not Pareto-optimal and they show deviations from the ground truth OCP solution as shown in section 4.1.

5. CONCLUSION

This work analyses the performance of model-predictive control (MPC) for dielectric elastomer generator-based wave energy converters under stochastic waves excitation. Compared to previous work, an MPC approach is considered for control, as it allows accounting for wave-by-wave changes in the excitation, while still accounting for energetic and damage cost functions. The MPC considerably deviates from ground truth solutions obtained by solving an optimum control problem (OCP) over an extremely long time frame, unless the prediction horizon covers a sufficiently large number of wave periods. As the sea state changes over time, the shape of the OCP Pareto front changes. As this makes achieving long-term objectives difficult, we propose a heuristic controller for selecting weight combinations that allow shifting the expected failure of the generator towards a target time in the future.

REFERENCES

Andersson, J.A., Gillis, J., Horn, G., Rawlings, J.B., and Diehl, M. (2019). Casadi: a software framework for nonlinear optimization and optimal control. *Mathematical Programming Computation*, 11(1), 1–36. doi:10.1007/s12532-018-0139-4.

Chen, Y., Agostini, L., Moretti, G., Berselli, G., Fontana, M., and Vertechy, R. (2019). Fatigue life performances of silicone elastomer membranes for dielectric elastomer transducers: preliminary results. In *Electroactive Polymer Actuators and Devices XXI*, volume 10966, 1096616. International Society for Optics and Photonics.

Coe, R.G., Bacelli, G., Cho, H., and Nevarez, V. (2018). A comparative study on wave prediction for wecs. Technical report, Sandia National Lab.(SNL-NM), Albuquerque, NM (United States).

Dissado, L.A. and Fothergill, J.C. (1992). *Electrical degradation and breakdown in polymers*, volume 9. Iet.

Duan, G.R. and Yu, H.H. (2013). Lmis in control systems. *CRC press*.

Faedo, N., Olaya, S., and Ringwood, J.V. (2017). Optimal control, mpc and mpc-like algorithms for wave energy systems: An overview. *IFAC Journal of Systems and Control*, 1, 37–56.

Gerdts, M. (2011). *Optimal Control of ODEs and DAEs*. Walter de Gruyter.

Hoffmann, M.K., Moretti, G., Rizzello, G., and Flaßkamp, K. (2022). Multi-objective optimal control for energy extraction and lifetime maximisation in dielectric elastomer wave energy converters. *IFAC-PapersOnLine*, 55(20), 546–551.

Moretti, G., Forehand, D., Vertechy, R., Fontana, M., and Ingram, D. (2014). Modeling of an oscillating wave surge converter with dielectric elastomer power take-off. In *International Conference on Offshore Mechanics and Arctic Engineering*, volume 45530, V09AT09A034. American Society of Mechanical Engineers.

Moretti, G., Herran, M.S., Forehand, D., Alves, M., Jeffrey, H., Vertechy, R., and Fontana, M. (2020). Advances in the development of dielectric elastomer generators for wave energy conversion. *Renewable and Sustainable Energy Reviews*, 117, 109430.

Pecher, A. and Kofoed, J.P. (2017). *Handbook of ocean wave energy*. Springer Nature.

Rawlings, J.B., Mayne, D.Q., and Diehl, M. (2017). *Model predictive control: theory, computation, and design*, volume 2. Nob Hill Publishing Madison, WI.

Requate, N., Meyer, T., and Hofmann, R. (2022). From wind conditions to operational strategy: Optimal planning of wind turbine damage progression over its lifetime. *Wind Energy Science Discussions*, 1–51.

Wächter, A. and Biegler, L.T. (2006). On the implementation of an interior-point filter line-search algorithm for large-scale nonlinear programming. *Mathematical programming*, 106(1), 25–57.

Whittaker, T. and Folley, M. (2012). Nearshore oscillating wave surge converters and the development of oyster. *Philosophical Transactions of the Royal Society A: Mathematical, Physical and Engineering Sciences*, 370(1959), 345–364.

Yu, Z. and Falnes, J. (1995). State-space modelling of a vertical cylinder in heave. *Applied Ocean Research*, 17(5), 265–275.